



Cu doped ZnO hierarchical nanostructures: morphological evolution and photocatalytic property

Qun Ma¹ · Xudong Yang¹ · Xiangzhou Lv¹ · Hanxiang Jia¹ · Yongqian Wang¹ 

Received: 26 September 2018 / Accepted: 3 December 2018 / Published online: 8 December 2018
© Springer Science+Business Media, LLC, part of Springer Nature 2018

Abstract

Copper doped ZnO hierarchical nanostructures have been synthesized with a facile solution route at room temperature. Structural properties of the as-synthesized nanostructures have been studied X-ray diffraction, field emission scanning electron microscopy with energy dispersive. Meanwhile, light-absorption properties were studied with UV–Vis absorption spectroscopy. Photocatalytic performance of Cu-doped ZnO hierarchical nanostructures were evaluated by the light-driven degradation of methylene blue. The results indicated that Cu doping lead to the augment of average crystallite size of ZnO crystals. Moreover, morphological evolution of ZnO nanostructures was found with the addition of Cu ions. The photocatalytic test showed that there is an optimum Cu doping concentration which results in the enhancement of photocatalytic performance of Cu doped ZnO hierarchical nanostructures, compared with pristine ZnO. A novel and reasonable mechanism was proposed. It is believed that the enhanced photocatalytic performance of Cu doped ZnO hierarchical nanostructures can be attributed to the formation of acceptor level ($\text{Cu}^{2+}\text{-Cu}^+$) in the midgap of ZnO, which improved the utilization of light and separation efficiency of photogenerated electron hole pairs.

1 Introduction

Zinc oxide (ZnO), a direct wide band gap (3.37 eV) semiconductor with a large electron–hole binding energy of 60 meV at room temperature, has attracted considerable attention in solar cells, light emitting diodes, ultraviolet lasers, water splitting, organic degradation, and so on, due to its distinctive and fascinating properties [1–4]. Over the past years, a wide range of ZnO nanostructures have been synthesized via various protocols [5–9]. For example, Yang et al. [10] synthesized hierarchical carbon-coated ZnO quantum dots by a one-step controlled pyrolysis of the metal–organic framework and investigated its outstanding electrochemical performance. Wang et al. [11] reported the synthesis of ZnO nanowires on both rigid and flexible using a low temperature solution method and investigated their piezotronic effect. Zhang et al. [12] fabricated nanosheet-assembled hierarchical flower-like ZnO nanostructures via

an ethanol-assisted hydrothermal route and studied their sensing properties towards acetone. Li et al. [13] prepared the flower-like ZnO microstructures by a one-step hydrothermal method and investigated their photocatalytic activity. Currently, the structure and properties of ZnO materials are still a research hot.

Semiconductor photocatalysts is of great importance to solve the current energy and environmental crises facing the modern industrial development [14–16]. ZnO, as an important semiconductor photocatalysts, has a huge potential to solve the above-mentioned problems [17]. However, the low utilization of sunlight and easy recombination of photoinduced electron–hole pairs of pristine ZnO materials limit its application as high effective photocatalysts. Hence, many groups focus on the improvement of photocatalytic activity of ZnO. Metal ions doping (Cu, Mn, etc.) has been demonstrated to be an effective means of controlling the band gap and absorption to improve the utilization of solar light [18, 19]. Moreover, the doping transition metal ions can alter the charge separation and recombination dynamics by creating electronics states in the midgap region, which is in favour of the enhancement of the photocatalytic activity [20–22]. There are some reports about the study of Cu doped ZnO nanostructures. For example, Liang et al. [23] synthesized Cu doped ZnO microstructures by a hydrothermal

✉ Yongqian Wang
cugwyq@126.com

¹ Engineering Research Center of Nano-Geomaterials of Ministry of Education, Faculty of Materials Science and Chemistry, China University of Geosciences, Wuhan 430074, China

method and studied their optical and photocatalytic properties. Lee et al. [24] reported the synthesis of Cu doped ZnO microstructures using a single-step chemical method and investigated their visible-light-driven photocatalytic performance. Mohapatra et al. [25] synthesized Cu doped ZnO nanostructures by a facile wet chemical method and found it that the obtained samples exhibited enhanced photocatalytic activity compared with pristine ZnO. The above exciting achievements motivate us to investigate the synthesis of Cu doped ZnO nanomaterials and their enhanced properties. Besides, to the best of our knowledge, we find it that the effect of Cu ions in the ZnO matrix on the energy band and properties of ZnO is still unclear. In other words, the mechanism of enhanced photocatalytic activity of Cu doped ZnO is unclear. Hence, it is essential and meaningful for us to systematically investigate the effect and photocatalytic mechanism.

In the work, Cu-doped ZnO hierarchical nanostructures have been synthesized with a facile wet chemical route at room temperature. The structural parameters of Cu-doped ZnO were investigated by XRD analysis and relative calculation. The morphological evolution was studied by the FESEM. The light-absorption of Cu doped ZnO hierarchical nanostructures was recorded with UV–Vis spectra. The photocatalytic performance was evaluated through measuring the degradation efficiency of methylene blue with the presence of Cu doped ZnO photocatalysts. Moreover, we proposed a reasonable mechanism to explain why Cu doping can improve the photocatalytic performance of ZnO.

2 Experimental section

2.1 Materials

Zinc acetate dihydrate, copper acetate monohydrate, sodium hydroxide and sodium citrate (Sinopharm Chemical Reagent Co., Ltd., China) were employed to synthesize Cu doped ZnO hierarchical nanostructures. All the reagents used in the present investigation were of analytical grade and used without further purification throughout the whole experimental process. Deionized water was used for preparation of all solutions.

2.2 Synthesis of Cu doped ZnO hierarchical nanostructures

For the synthesis of ZnO nanostructures, 0.1 M of zinc acetate dehydrate and citrate (0.24 M) were dissolved into 60 mL deionized water under stirring to form a transparent solution. And then sodium hydroxide (NaOH) with the concentration that is five times higher than that of Zn^{2+} concentration was slowly dropped into the transparent solution

under constantly stirring which was continued for 2 h at room temperature (25 °C). Finally, the white samples were obtained by centrifugation, repeatedly washed with deionized water and anhydrous ethanol to remove impurities, and dried overnight in an oven at 60 °C in air.

For the synthesis of Cu doped ZnO nanostructures, appropriate amounts of copper acetate monohydrate was added into the solution containing 0.1 M of zinc acetate dehydrate, citrate (0.24 M) and 0.5 M sodium hydroxide (NaOH), and the resulted solution was continued for 2 h at room temperature (25 °C). The relative amount of copper acetate monohydrate in the solution was varied as 1.5%, 3.0% and 5% with respect to the molar ratio of Cu/Zn.

2.3 Characterization

The synthesized samples were characterized with multiple technologies. The general morphology of the synthesized samples was investigated with field emission scanning electron microscopy (FESEM, SU8010, HITACHI). The samples were pretreated with a thin amorphous gold on their surface before FESEM analysis. The element composition of the samples was measured with energy dispersive X-ray spectrometer (EDS) attached to the FESEM. The structure and crystal phase of the samples were characterized by powder X-ray diffraction (XRD, D8 Advanced XRD, Bruker-AXS). UV–Vis diffuse reflectance spectra were recorded with an UV–Vis spectrophotometer (UV-3600, Shimadzu, Tokyo, Japan). The room-temperature photoluminescence (PL) spectra of the samples were measured by fluorescence spectrophotometer (F-4500, HITACHI).

2.4 Photocatalytic tests

Photocatalytic performance of as-synthesized samples was evaluated through measuring the degradation efficiency of methylene blue with the presence of photocatalysts. Before photocatalytic test, all mixed solution with photocatalysts and methylene blue were placed in dark environment for 1 h to reach adsorption equilibrium, and then the residual concentration of methylene blue was measured. In a typical experiment, a 250 W high pressure mercury lamp was used as light source. The lamp was placed 8 cm above the liquid surface. Subsequently, 0.1 g of photocatalysts was added into a 100 mL of 1×10^{-5} M methylene blue aqueous solution. The mixed solution was stirred constantly in the process of experiment. For a given duration (30 min), 3 mL solution was extracted to test the residual concentration of methylene blue, which was evaluated by measuring the change of maximum absorbance in the UV–Vis spectrometry (UV-3600, Shimadzu). The absorbent peak in about 664 nm was selected and the residual concentration was obtained though evaluating the intensity ratio between remained and original

MB solution. The degradation rate was calculated as following equation:

$$\text{Photocatalytic efficiency (\%)} = (C_0 - C)/C_0 \times 100\%$$

where C is the concentration of methylene blue at each irradiated time, and C_0 is the initial concentration when adsorption–desorption equilibrium is achieved.

3 Results and discussions

3.1 Crystal structure and morphology

Figure 1 shows the XRD patterns of as-synthesized Cu-doped ZnO hierarchical nanostructures with varying molar ratio of Cu/Zn. The diffraction peaks of pristine ZnO crystals are indexed to the diffraction faces of (100), (002), (101), (102), (110), (103), (200), (112) and (201), respectively, which correspond to the hexagonal wurtzite ZnO structure with $a=0.32493$ nm and $c=0.52076$ nm (JCPDS No. 05-0664). The addition of low Cu concentration dopants in ZnO leads to no significant shift of diffraction peaks, which could be attributed to the ionic radii of Cu^{2+} (0.057 nm) is close to that of Zn^{2+} (0.060 nm). It is noteworthy to mention that extra peaks were indexed in the case of sample synthesized with high Cu concentration (5.0%), corresponding to the monoclinic CuO structure (JCPDS No. 02-1040). The results confirm the formation of CuO in the ZnO crystals. However, the intensity of CuO is so low that we can ignore it when we perform the low concentration doping. According to the Scherrer equation, the average crystallite sizes of obtained ZnO were estimated to be 20.62 nm, 28.84 nm,

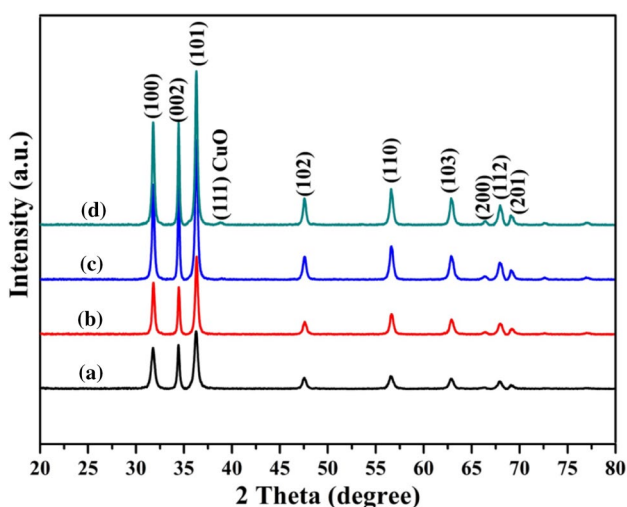


Fig. 1 XRD patterns of the as-synthesized Cu doped ZnO hierarchical nanostructures with varying molar ratio of Cu/Zn, (a) 0%, (b) 1.5%, (c) 3.0%, (d) 5.0%

31.15 nm and 25.16 nm for the 0%, 1.5%, 3.0% and 5.0% of Cu doped ZnO hierarchical nanostructures.

Figure 2 shows the representative FESEM images of as-synthesized Cu doped ZnO hierarchical nanostructures. The pristine ZnO has uniform flower-like hierarchical nanostructures assembled by a large number of nanosheets with irregular arrangement. The nanosheets interact with each other, leading to a porous net-like structure. It is of special interest to observe that the morphological evolution of ZnO occurs with the increasing concentration of Cu ions. When the molar ratio of Cu/Zn is 1.5%, the obtained Cu doped ZnO (Cu–ZnO-1.5) presents similar flower-like structure from the whole view. However, the inner structure of “flower” is different with pristine ZnO. The hierarchical structure is assembled by nanosheets and nanoparticles. The nanoparticles locate in the surface of nanosheets. With the increasing concentration of Cu ions, the obtained Cu doped ZnO (Cu–ZnO-3.0) exhibits another hierarchical structure. The component of hierarchical structure has further been transited to nanorods. Compared with Cu–ZnO-1.5, nanorods form and nanoparticles disappear. When the molar ratio of Cu/Zn is up to 5.0%, the hierarchical nanostructures are completely assembled by nanorods with irregular arrangement and different growth direction.

The chemical composition of the pristine ZnO and Cu doped ZnO hierarchical structure (Cu–ZnO-3.0) was investigated by the EDS. As shown in Fig. 3, the left is the EDS spectrum of pristine ZnO, and the right is that of Cu doped ZnO hierarchical structure. The EDS spectrum (left) only shows the presence of Zn and O. The right spectrum is composed of Zn, O and Cu, indicating that the presence of Cu in the ZnO.

It should be very meaningful to understand why and how the morphology transforms. In the case, the addition of Cu ions is critical for the morphological transition [26]. Pure ZnO hierarchical nanostructures are assembled by nanosheets. It is well known that the growth of ZnO crystal is very sensitive to the compositional change of the initial environment. When the Cu ions were added into the reaction solution, it would change the crystal growth environment and produce defects in the initial ZnO crystals. When the molar ratio of Cu/Zn is 1.5%, the hierarchical nanostructures are composed of nanosheets and nanoparticles. The formation of nanoparticles could be attributed to the secondary growth of ZnO crystals. When the molar ratio is 3.0%, the obtained hierarchical nanostructures are composed of nanorods. It is well known that ZnO has polar-terminated (0001) and nonpolar low-symmetry (10–10) faces [27]. Naturally, ZnO crystal tends to growth along the [0001] direction. Besides, excessive Cu ions will be absorbed on the surface of nonpolar low-symmetry faces, leading to the formation of nanorods. When the molar ratio is up to 5%, the addition of Cu ions causes some defects in the primary

Fig. 2 FESEM images of the as-synthesized Cu doped ZnO hierarchical nanostructures with varying molar ratio of Cu/Zn, **a**, **b** 0%, **c**, **d** 1.5%, **e**, **f** 3.0%, (**g**, **h**) 5.0%

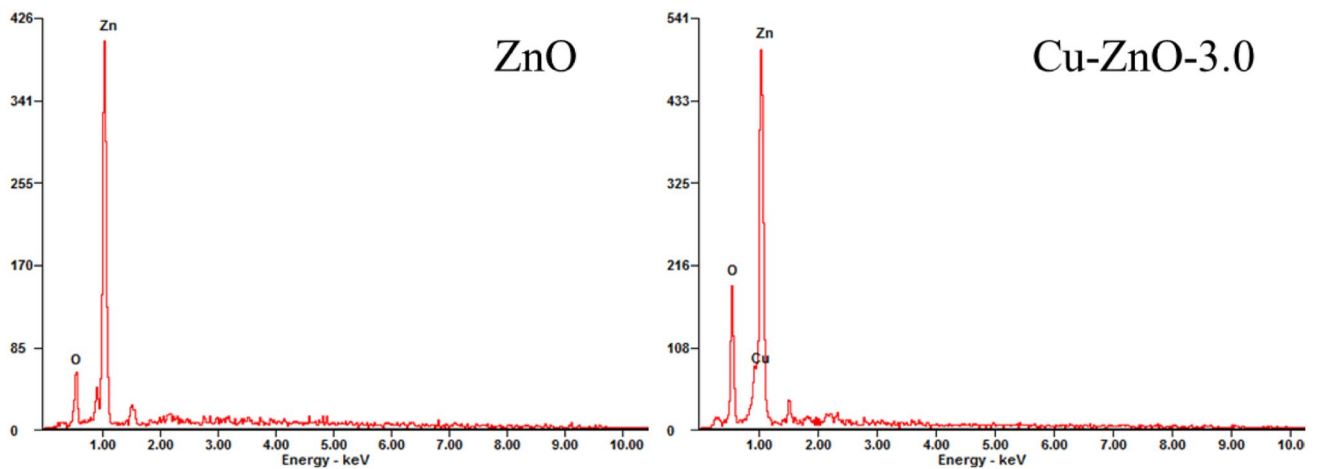
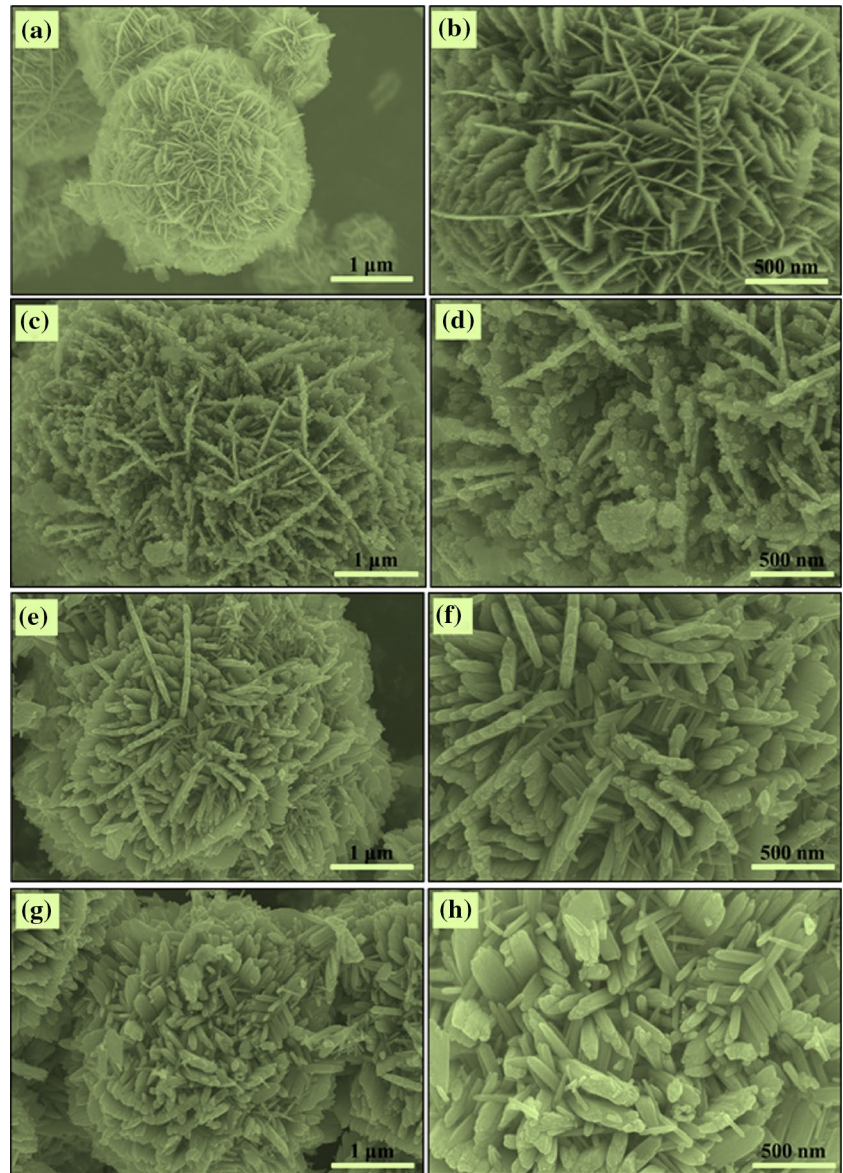


Fig. 3 EDS spectra of ZnO (left) and Cu doped ZnO (right)

nanorods and secondary nanorods form, resulting in the formation of branch-like structure. The morphological evolution is shown in Fig. 4.

3.2 Optical properties

The UV–Vis absorption spectra of obtained Cu doped ZnO hierarchical nanostructures were recorded in the wavelength range of 250–800 nm, as shown in Fig. 5a. The incorporation of Cu into ZnO matrix leads to the enhanced absorption in the visible light, improving the utilization of sunlight. The enhancement could be attributed to acceptor level due to the incorporation of Cu. It is known that the optical band gap (E_g) can be estimated according to the Tauc plot [28]:

$$\alpha h\nu = (h\nu - E_g)^n$$

where α is the optical absorption coefficient, h is the Planck constant, ν is the photon frequency, E_g is optical band gap and n is a parameter associated with the type of electronic transition: $n = 1/2$ for a direct allowed transition (for example, ZnO, ZnS) and $n = 2$ for an indirect allowed transition.

To investigate the effect of the addition of Cu on the band gap of ZnO, $(\alpha h\nu)^2$ versus $(h\nu)$ plot was made (Fig. 5b). The value of band gap (E_g) can be estimated by extrapolating the linear portion of the plot of $(\alpha h\nu)^2$ versus $h\nu$ to $(\alpha h\nu)^2 = 0$. The estimated values of the optical band gap for Cu doped ZnO hierarchical nanostructures with varying Cu/Zn molar ratio are 3.24 eV, 3.21 eV, 3.20 eV, and 3.17 eV, respectively.

The photocatalytic activity of all samples was evaluated by degradation of methylene blue (MB) in aqueous solution under UV–Vis irradiation. The reduction of MB due to the adsorption on the surface of photocatalysts was ignored. As shown in Fig. 6, when photocatalysts were absent, the concentration of methylene blue (MB) did not reduce, indicating that MB molecules will not be decomposed without the photocatalysts. It can be observed that photocatalytic efficiency increases with the increasing of reaction time. After 240 min, pristine ZnO only degraded 70% of MB. For the Cu doped ZnO hierarchical nanostructures exhibit an obvious enhancement of photodegradation, compared with pristine ZnO. The photocatalytic efficiency can reach up to 95% after 240 min. Moreover, it can be observed based on the results

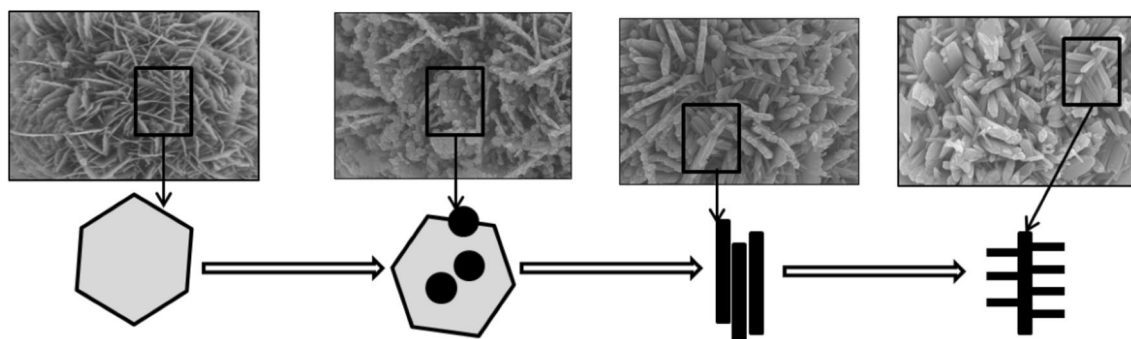


Fig. 4 Schematic presentation of the morphological transition of Cu doped ZnO hierarchical structures

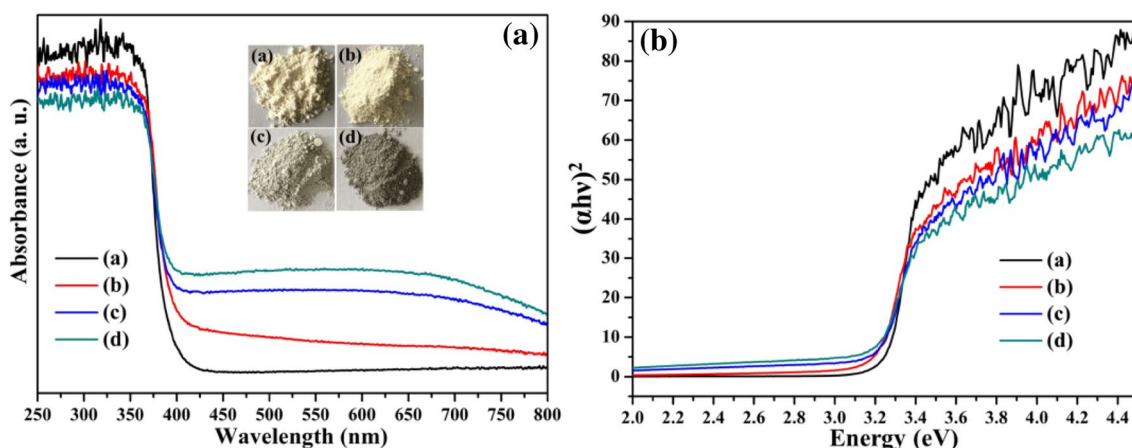


Fig. 5 **A** UV–Visible absorption spectra and **B** $(\alpha h\nu)^2$ versus $h\nu$ plots of Cu doped ZnO nanostructures with varying molar ratio of Cu/Zn, (a) 0%, (b) 1.5%, (c) 3.0%, (d) 5.0%

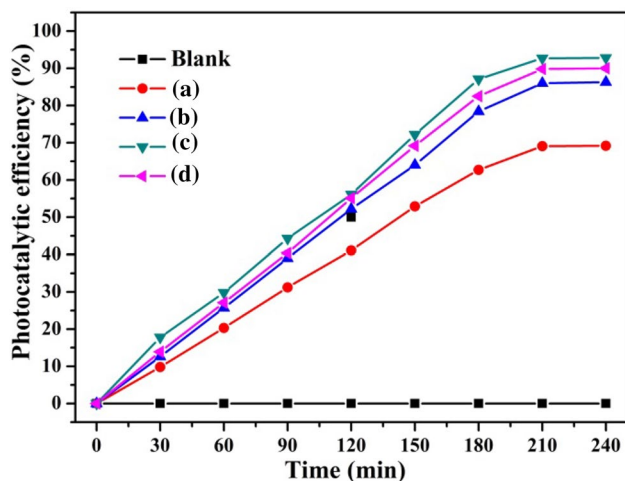


Fig. 6 Photocatalytic activity of the as-synthesized Cu doped ZnO hierarchical nanostructures with varying molar ratio of Cu/Zn, (a) 0%, (b) 1.5%, (c) 3.0%, (d) 5.0%

that there is an optimal level of Cu doping in ZnO which leads to the most efficient photocatalytic performance. In the case, the ZnO hierarchical with 3.0% of Cu doping presents the most efficient photocatalytic activity.

It is known that the performance of photocatalysts depends on two conditions: (a) the high utilization of light and (b) the limited recombination of photoinduced electron–hole pairs. For the pristine ZnO, its photocatalytic performance is low because of its narrow light-absorption range and fast recombination of electron–hole pairs. However, for the Cu-doped ZnO, when the Cu ions enter into the ZnO matrix, it will not only produce acceptor level which can use as electron acceptor and limit the recombination of photogenerated electron–hole pairs in the photodegradation process, but also change the inner environment of ZnO crystal which could adjust the band structure and enhance the light absorption [29]. A reasonable mechanism has been proposed to explain the process of how the acceptor level of Cu ions function. Initially, when the Cu doped ZnO photocatalysts is exposed to the light, the photoinduced electrons and holes form. Initially, the photoinduced electrons migrate to the conduction band (CB), and the photoinduced holes stay at valence band (VB). Driven the potential energy, the electrons will return to the VB from the CB for the pristine ZnO. However, for the Cu doped ZnO, the electron will be accepted by the acceptor level of Cu^{2+} . When the Cu^{2+} accepts the electron, it will be reduced to Cu^+ [30, 31]. Due to the reduction process, the lifespan of photoinduced holes are extended and the electron–hole pairs are effectively separated. Hence, it is not difficult to understand why the photocatalytic performance of Cu doped ZnO is better than that of the pristine ZnO. Subsequently, surface hydroxyl groups react with

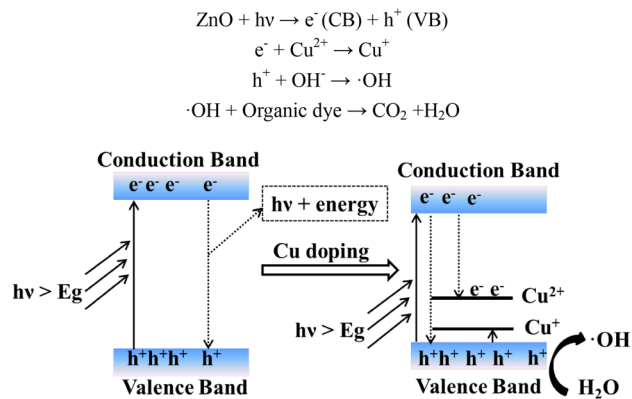
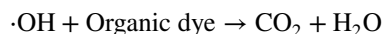
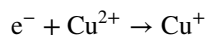
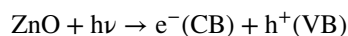


Fig. 7 Photocatalytic mechanism of Cu doped ZnO hierarchical nanostructures

holes in the valence band of ZnO resulting to the formation of reactive hydroxyl ($\cdot\text{OH}$) radicals. Finally, the $\cdot\text{OH}$ which has strong oxidation react with the organic molecules absorbed on the surface of ZnO, leading to their degradation. The mechanism was schematically shown in Fig. 7 and the corresponding reactions are as follows.



4 Conclusions

In conclusion, Cu-doped ZnO hierarchical nanostructures were synthesized with wet chemical route at room temperature. It was found that the average crystallite size increased due to the incorporation of Cu ions into ZnO matrix. With the increasing of Cu concentration, the hierarchical nanostructures were initially assembled by nanosheets, transforming into nanosheets and then nanoparticles, finally nanorods. The initial addition of Cu ions could affect the crystal growth of primary ZnO leading to the morphological evolution. Moreover, the incorporation of Cu also enhanced the visible-light absorption of ZnO by adjusting its structure of energy band. The E_g value decreased with the increasing of Cu concentration. The photocatalytic performance of Cu doped ZnO hierarchical nanostructures exhibited significant enhancement, which could be attributed to the reduction of Cu^{2+} into Cu^+ causing the effective separation of photogenerated electrons–hole pairs.

Acknowledgements Y. Q. Wang designed and directed the project. Q. Ma and X. D. Yang carried out the experiments, performed measurements and carried out data analysis with help from X. Z. Lv and H. X. Jia, and Y. Q. Wang wrote the manuscript. All authors contributed to discussions. The project was supported by the Fundamental Research Funds for National Universities, China University of Geosciences (Wuhan).

References

- S. Dutta, S. Chattopadhyay, A. Sarkar, M. Chakrabarti, D. Sanyal, D. Jana, Role of defects in tailoring structural, electrical and optical properties of ZnO. *Prog. Mater. Sci.* **54**, 89–136 (2009)
- A.B. Djurišić, X. Chen, Y.H. Leung, A.M.C. Ng, ZnO nanostructures: growth, properties and applications. *J. Mater. Chem.* **22**, 6526–6535 (2012)
- J.C. Fan, K. Srekanth, Z. Xie, S. Chang, K.V. Rao, p-Type ZnO materials: theory, growth, properties and devices. *Prog. Mater. Sci.* **58**, 874–985 (2013)
- S. Maiti, S. Pal, K.K. Chattopadhyay, Recent advances in low temperature, solution processed morphology tailored ZnO nanoarchitectures for electron emission and photocatalysis applications. *CrystEngComm* **17**, 9264–9295 (2015)
- Z.R. Tian, J.A. Voigt, J. Liu, B. Mckenzie, M.J. Mcdermott, M.A. Rodriguez, H. Konishi, H. Xu, Complex and oriented ZnO nanostructures. *Nat. Mater.* **2**, 821 (2003)
- S. Baruah, J. Dutta, Hydrothermal growth of ZnO nanostructures. *Sci. Technol. Adv. Mater.* **10**, 013001 (2009)
- A. Wei, L. Pan, W. Huang, Recent progress in the ZnO nanostructure-based sensors. *Mater. Sci. Eng. B* **176**, 1409–1421 (2011)
- S. Xu, Z.L. Wang, One-dimensional ZnO nanostructures: solution growth and functional properties. *Nano Res.* **4**, 1013–1098 (2011)
- Y. Wang, Q. Ma, H. Jia, Z. Wang, One-step solution synthesis and formation mechanism of flower-like ZnO and its structural and optical characterization. *Ceram. Int.* **42**, 10751–10757 (2016)
- S.J. Yang, S. Nam, T. Kim, J.H. Im, H. Jung, J.H. Kang, S. Wi, B. Park, C.R. Park, Preparation and exceptional lithium anodic performance of porous carbon-coated ZnO quantum dots derived from a metal–organic framework. *J. Am. Chem. Soc.* **135**, 7394–7397 (2013)
- K.C. Pradel, W. Wu, Y. Zhou, X. Wen, Y. Ding, Z.L. Wang, Piezotronic effect in solution-grown p-type ZnO nanowires and films. *Nano Lett.* **13**, 2647–2653 (2013)
- X. Luo, Z. Lou, L. Wang, X. Zheng, T. Zhang, Fabrication of flower-like ZnO nanosheet and nanorod-assembled hierarchical structures and their enhanced performance in gas sensors. *New J. Chem.* **38**, 84–89 (2014)
- Y. Su, J. Li, Z. Luo, B. Lu, P. Li, Microstructure, growth process and enhanced photocatalytic activity of flower-like ZnO particles. *RSC Adv.* **6**, 7403–7408 (2016)
- J. Zhang, P. Liu, Y. Zhang, G. Xu, Z. Lu, X. Wang, Y. Wang, L. Yang, X. Tao, H. Wang, Enhanced performance of nano-Bi₂WO₆-graphene as pseudocapacitor electrodes by charge transfer channel. *Sci. Rep.* **5**, 8624 (2015)
- Q. Ma, Y. Wang, J. Kong, H. Jia, Tunable synthesis, characterization and photocatalytic properties of various ZnS nanostructures. *Ceram. Int.* **42**, 2854–2860 (2016)
- J. Zhang, B. Wu, L. Huang, P. Liu, X. Wang, Z. Lu, G. Xu, E. Zhang, H. Wang, Z. Kong, Anatase nano-TiO₂ with exposed curved surface for high photocatalytic activity. *J. Alloy. Compd.* **661**, 441–447 (2016)
- J. Yang, H. Jia, X. Lv, Y. Wang, Facile preparation of urchin-like ZnO nanostructures and their photocatalytic performance. *Ceram. Int.* **42**, 12409–12413 (2016)
- M. Ahmad, E. Ahmed, Z. Hong, X. Jiao, T. Abbas, N. Khalid, Enhancement in visible light-responsive photocatalytic activity by embedding Cu-doped ZnO nanoparticles on multi-walled carbon nanotubes. *Appl. Surf. Sci.* **285**, 702–712 (2013)
- F. Achouri, S. Corbel, L. Balan, K. Mozet, E. Girot, G. Medjahdi, M.B. Said, A. Ghrabi, R. Schneider, Porous Mn-doped ZnO nanoparticles for enhanced solar and visible light photocatalysis. *Mater. Des.* **101**, 309–316 (2016)
- L. Shen, R. Wu, H. Pan, G. Peng, M. Yang, Z. Sha, Y. Feng, Mechanism of ferromagnetism in nitrogen-doped ZnO: first-principle calculations. *Phys. Rev. B* **78**, 073306 (2008)
- G.Z. Xing, J.B. Yi, J.G. Tao, T. Liu, L.M. Wong, Z. Zhang, G.P. Li, S.J. Wang, J. Ding, T.C. Sum, Comparative study of room-temperature ferromagnetism in Cu-doped ZnO nanowires enhanced by structural inhomogeneity. *Adv. Mater.* **20**, 3521–3527 (2008)
- C. Xia, F. Wang, C. Hu, Theoretical and experimental studies on electronic structure and optical properties of Cu-doped ZnO. *J. Alloy. Compd.* **589**, 604–608 (2014)
- G. Liang, L. Hu, W. Feng, G. Li, A. Jing, Enhanced photocatalytic performance of ferromagnetic ZnO: Cu hierarchical microstructures. *Appl. Surf. Sci.* **296**, 158–162 (2014)
- R.C. Pawar, D.-H. Choi, J.-S. Lee, C.S. Lee, Formation of polar surfaces in microstructured ZnO by doping with Cu and applications in photocatalysis using visible light. *Mater. Chem. Phys.* **151**, 167–180 (2015)
- S. Kuriakose, B. Satpati, S. Mohapatra, Highly efficient photocatalytic degradation of organic dyes by Cu doped ZnO nanostructures. *Phys. Chem. Chem. Phys.* **17**, 25172–25181 (2015)
- Z. Zhang, J.B. Yi, J. Ding, L.M. Wong, H.L. Seng, S.J. Wang, J.G. Tao, G.P. Li, G.Z. Xing, T.C. Sum, Cu-doped ZnO nanoneedles and nanonails: morphological evolution and physical properties. *J. Phys. Chem. C* **112**, 9579–9585 (2008)
- G. Li, T. Hu, G. Pan, T. Yan, X. Gao, H. Zhu, Morphology—function relationship of ZnO: polar planes, oxygen vacancies, and activity. *J. Phys. Chem. C* **112**, 11859–11864 (2008)
- J. Tauc, Optical properties and electronic structure of amorphous Ge and Si. *Mater. Res. Bull.* **3**, 37–46 (1968)
- F. Zhang, X.-W. He, W.-Y. Li, Y.-K. Zhang, One-pot aqueous synthesis of composition-tunable near-infrared emitting Cu-doped CdS quantum dots as fluorescence imaging probes in living cells. *J. Mater. Chem.* **22**, 22250–22257 (2012)
- R. Xie, X. Peng, Synthesis of Cu-doped InP nanocrystals (d-dots) with ZnSe diffusion barrier as efficient and color-tunable NIR emitters. *J. Am. Chem. Soc.* **131**, 10645–10651 (2009)
- B.B. Srivastava, S. Jana, N. Pradhan, Doping Cu in semiconductor nanocrystals: some old and some new physical insights. *J. Am. Chem. Soc.* **133**, 1007–1015 (2010)